Journal of the Physical Society of Japan 85, 054001 (2016)
http://doi.org/10.7566/JPSJ.85.054001

Accuracy of Weak-Form Discretisation and Extention of Recursive Transfer Method for Scattering Problems Governed by Fourth-Order Differential Equation

Hatsuhiro Kato[1] and Hatsuyoshi Kato[2]

[1]*University of Yamanashi, Kofu 400-8511, Japan*
[2]*National Institute of Technology, Tomakomai College, Tomakomai, Hokkaido 059-1275, Japan*

(Received December 9, 2014; accepted February 22, 2016; published online April 25, 2016)

We proposed a new discretisation scheme for deriving a second-order difference equation from any system being formulated with the weak-form theory framework. The proposed scheme enables us to extend the application range of the recursive transfer method (RTM) and to express perfectly matching conditions for port boundaries in a discrete fashion under the RTM framework. To evaluate the accuracy and demonstrate the validity of the proposed scheme, we discussed the scattering problem governed by the fourth-order differential equation that was hitherto outside the RTM application range. The difference equation can play an important role in maintaining the balance of the bending moment and the shear force at the interface of two segments. Using the new port boundary condition, a quasi-localised wave was extracted and found to be related to the phase shift due to Fano resonance.

1. Introduction

Using a second-order difference equation derived by the Numerov method,[1] the recursive transfer method (RTM) has been developed to analyse electron conductance,[2,3] metallic polymers,[4] and microwave scattering.[5] RTM is a method of analysing the scattering problem and extracting a localised wave with a systematic procedure.[6] However, the differential equations to which the Numerov method is applicable are limited to the second order without the first derivative. Thus the application range of RTM is also limited.

To extend the application range of RTM, a new discretisation scheme was proposed on the basis of the weak-form theory framework; the limitation on the physical system to which RTM is applicable was removed. Furthermore, new expressions of port boundaries were also developed, which are consistent with the RTM procedure and termed as the RTM-consistent port boundary condition (PBC). This condition serves as the perfectly matching condition in discretised systems instead of an analytical expression that is strict in continuous systems but induces mismatching by discretisation.[7,8] The concept of perfect matching was proposed concerning electromagnetic systems[9,10] and it was also developed in elastodynamic systems.[11] Since the proposed RTM-consistent PBC has no need to prepare an artificial absorbing layer, localised/quasi-localised waves can be extracted with an eigenvalue problem even if a damping wave tail reaches the ends of the analysis domain.

The advantage of weak-form discretisation is its potentiality to extend RTM to various systems beyond the system governed by the second-order differential equation. To evaluate the accuracy and demonstrate the validity of the proposed scheme, we discussed a scattering problem governed by the fourth-order differential equation that was hitherto outside the RTM application range. The difference equation can play an important role in maintaining the balances of the bending moment and the shear force at the interface of two segments. By using the system that has a strict expression of the transmission rate, the discretisation error was investigated. The issues discussed in this study would lead to the development of a promising method of analysing problems in one-dimensional systems.

Recently, scattering phenomena in elastodynamic systems such as mesoscopic waveguides[12,13] and nanowires[14,15] have been attracted much attention. Although Fano resonance was discussed under a quasi-one-dimensional system by separating a wave motion into directions parallel and perpendicular to the propagation axis,[16] in a pure one-dimensional system governed by the second-order differential equation, any wave induced by an incident wave emits wave skirts to the input/output regions and does not form a stable localised wave. In a system governed by the fourth-order differential equation, Fano resonance does exist because a stable localised wave can exist. Fano resonance in a quasi-one-dimensional system has already been studied using the Green function method;[16] however, our method has the unique property that enables us to extract a localised/quasi-localised wave that causes Fano resonance.[17,18] A quasi-localised wave is related to the complex eigenvalue whose real part is the frequency and the imaginary part is the lifetime of the oscillation.

This paper is organized as follows: In Sect. 2, by introducing a fourth-order differential equation, the theoretical framework of weak-form discretisation is developed. In Sect. 3, the solution of a scattering problem with RTM is summarized. New stepping matrices in the input/output ports of a waveguide are defined; they play an important role in expressing the RTM-consistent PBC. In Sect. 4, the accuracy of weak-form discretisation is evaluated using the resonance curve. A new method of extracting the localised/quasi-localised wave is also proposed, and its application to estimating phase shift in Fano resonance is discussed. In Sect. 5, the results of this study are summarized. In Appendix, details of deriving the theoretical expression of transmission rate are summarized from the viewpoint of localised waves.

2. Weak-Form Discretisation for RTM

2.1 Functional

The elastic bar in flexural motion is governed by the fourth-order differential equation as[19]

$$\{\ell(x)u''\}'' - \tilde{m}(x)u + \ddot{u} = 0. \tag{1}$$

Here x is the space coordinate, $u(x)$ is the lateral displacement of the elastic bar, $\ell(x)$ and $\tilde{m}(x)$ are functions for determining system features. The notations $'$ and $\dot{}$ indicate derivatives with respect to space and time, respectively. When the system is in a steady oscillation state with the angular frequency ω, the dynamic term $\ddot{u}$ can be assumed to be $-\omega^2 u$, and it can be included in the new function $m(x)$ as $m(x) = \tilde{m}(x) + \omega^2$. The functional F_n for weak-form discretisation can be defined with the test function $w(x)$ as

$$F_n[w, u] = \int_{x_n-h}^{x_n+h} \{ w''\ell(x)u'' - wm(x)u \} \, dx. \tag{2}$$

The analysis domain between the input and output terminals, $x = x_{\rm in}$ and $x_{\rm out}$, was segmented into N elements as follows: $x_n = x_{\rm in} + hn$, where $n\ (= 0, 1, 2, \ldots, N)$ is the site index and h is the step size defined by $h = (x_{\rm out} - x_{\rm in})/N$. By separating the integration interval of Eq. (2) into two parts $[x_n - h, x_n]$ and $[x_n, x_n + h]$ and regarding the function $\ell(x)u''(x)$ $(= v(x))$ to be not always continuous at $x = x_n$, we can transform Eq. (2) as

$$\begin{aligned} F_n[w, u] = &\int_{x_n-h}^{x_n+h} w\{(\ell(x)u'')'' - m(x)u\} \, dx \\ &+ [w'(x)v(x) - w(x)v'(x)]_{x_n-h}^{x_n+h} \\ &+ w'(x_n)\{ v(x_n - 0) - v(x_n + 0)\} \\ &- w(x_n)\{ v'(x_n - 0)) - v'(x_n + 0)\}, \end{aligned} \tag{3}$$

where $v(x_n \pm 0)$ indicates the limit $\lim_{\epsilon\to 0} v(x_n \pm \epsilon)$ that maintains the condition $\epsilon > 0$.

From the first term of the right hand side in Eq. (3), Eq. (1) can be derived by the null value problem defined as what $u(x)$ satisfies $F_n[w, u] = 0\ (\forall w)$. When the test function $w(x)$ satisfies the restrictions as

$$w(x_n \pm h) = 0, \quad w'(x_n \pm h) = 0, \tag{4}$$

boundary terms of $v(x_n \pm h)$ and $v'(x_n \pm h)$ appearing in the second term of Eq. (3) are eliminated and we can impose any boundary condition at the input/output ports according to the behaviour of scattering waves. Furthermore, we can also impose the condition that $v(x)$ and $v'(x)$ must be continuous at the boundary $x = x_n$ because the values $w(x_n)$ and $w'(x_n)$ are arbitrary in the third and fourth terms of Eq. (3). These imply the condition in which the bending moment and shear stress must maintain balance at the interface of the segments. This is one of the important roles of the difference equation. Using these features included in the functional expression, we can transform the differential equation into the difference equation as shown in the following section.

2.2 *Interpolation of field variables*

The second-order difference equation can be derived by expressing Eq. (2) through the interpolation of fields at three successive points. One of the suitable interpolation tools is provided by the Hermite element developed in FEM.[19] Using the 4×4 matrix $C_\pm$ defined as

$$C_\pm = \begin{bmatrix} 1 & 0 & 0 & 0 \\ 0 & 1 & 0 & 0 \\ 1 & \pm h & h^2 & \pm h^3 \\ 0 & 1 & \pm 2h & 3h^2 \end{bmatrix}^{-1}, \tag{5}$$

we can interpolate the field $u(x)$ with cubic polynomials of the variable $\xi\ (= x - x_n \in [-h, h])$ as

$$u(x) = \begin{cases} \{\xi\} C_- [\mathbf{u}(x_n)^{\rm T}, \mathbf{u}(x_{n-1})^{\rm T}]^{\rm T} & -1 < \xi < 0 \\ \{\xi\} C_+ [\mathbf{u}(x_n)^{\rm T}, \mathbf{u}(x_{n+1})^{\rm T}]^{\rm T} & 0 < \xi < 1 \end{cases}. \tag{6}$$

Here the sybol T means the transpose, $\{\xi\}$ is a shorten expression for the four-dimensional row vector defined by $\{\xi\} = [1, \xi, \xi^2, \xi^3]$, and $\mathbf{u}(x_n)$ is two-dimensional field vector $\mathbf{u}(x) = [u(x), u'(x)]^{\rm T}$.

The test function $w(x)$ can also be interpolated with two-dimensional vector $\mathbf{w}(x) = [w(x), w'(x)]^{\rm T}$ as follows:

$$w(x) = \begin{cases} \{\xi\} C_- R_- \mathbf{w}(x_n) & -1 < \xi < 0 \\ \{\xi\} C_+ R_+ \mathbf{w}(x_n) & 0 < \xi < 1 \end{cases}, \tag{7}$$

where the boundary conditions (4) was used, and 4×2 matrix $R_\pm$ is defined as $R_\pm = [I, O]^{\rm T}$ with 2×2 identity and zero matrices, I and O, respectively.

2.3 *Second-order difference equation*

Using Eqs. (6) and (7), the functional (2) can be transformed into

$$F_n = \mathbf{w}(x_n)^{\rm T} \sum_{\sigma=\pm} R_\sigma^{\rm T} f_{n\sigma} [\mathbf{u}(x_n)^{\rm T}, \mathbf{u}(x_{n+\sigma 1})^{\rm T}]^{\rm T}, \tag{8}$$

where $f_{n\sigma}$ is a 4×4 matrix defined by

$$f_{n\sigma} = \ell\left(x_n + \frac{\sigma h}{2}\right) A_\sigma - m\left(x_n + \frac{\sigma h}{2}\right) B_\sigma, \tag{9}$$

with

$$A_\sigma = C_\sigma^{\rm T} \int_{-h}^{h} \{\xi\}''^{\rm T} \{\xi\}'' \, d\xi \, C_\sigma, \tag{10}$$

$$B_\sigma = C_\sigma^{\rm T} \int_{-h}^{h} \{\xi\}^{\rm T} \{\xi\} \, d\xi \, C_\sigma. \tag{11}$$

Here the functions $m(x)$ and $\ell(x)$ are expressed with the constant values $m(x_n + h/2)$ and $\ell(x_n + h/2)$ in the interval $[x_n, x_{n+1}]$ to reflect the stepwise change assumed in Sect. 4.1. It is also possible to use the polynomial interpolation function if the functions $m(x)$ and $\ell(x)$ are continuous. The null value problem yields the second-order difference equation as

$$c_n \mathbf{u}(x_{n-1}) + b_n \mathbf{u}(x_n) + a_n \mathbf{u}(x_{n+1}) = \mathbf{0}, \tag{12}$$

where c_n, b_n, and a_n are 2×2 matrices defined by

$$c_n = R_-^{\rm T} f_{n-} [O, I]^{\rm T}, \tag{13}$$

$$b_n = (R_-^{\rm T} f_{n-} + R_+^{\rm T} f_{n+})[I, O]^{\rm T}, \tag{14}$$

$$a_n = R_+^{\rm T} f_{n+} [O, I]^{\rm T}. \tag{15}$$

Under the RTM framework, the field vectors $\mathbf{u}(x_n)$ are assumed to be transferred according the rule

$$\mathbf{u}(x_{n+1}) = S_n \mathbf{u}(x_n). \tag{16}$$

Here S_n is the 2×2 matrix that was termed as the stepping matrix[2] or the recursion matrix.[3] Equations (16) and (12) yield

$$S_{n-1} = -(b_n + a_n S_n)^{-1} c_n. \tag{17}$$

If the terminal value S_N is given, all values of S_n $(n < N)$ can be obtained by the successive use of Eq. (17) [see Eq. (23) in Sect. 3.1.2].

3. Scattering Problem

3.1 RTM

3.1.1 Discretised modes in port and stepping matrices

Let us consider the scattering problem caused by an incident wave coming from $x = -\infty$ and scattered in the region $x_{\rm in} < x < x_{\rm out}$. The incident wave involves a reflection wave and a transmission wave in the input port region, $x < x_{\rm in}$ ($n < 0$), and the output port region, $x > x_{\rm out}$ ($n > N$), respectively.

RTM is a numerical method of connecting various waves generated in the scattering region to the wave modes in the port region. When the input/output port region is assumed to be extended to an infinite and uniform space, the coefficients in Eq. (12) can be regarded as independent of n. Therefore, using the constant coefficients $c_{\rm prt}$, $b_{\rm prt}$, and $a_{\rm prt}$ which show no n dependence, we can put $c_n = c_{\rm prt}$, $b_n = b_{\rm prt}$, and $a_n = a_{\rm prt}$ in extended port regions. Here the constants $c_{\rm prt}$, $b_{\rm prt}$, and $a_{\rm prt}$ are respectively defined by Eqs. (13), (14), and (15) at any site in the port regions. Then, the solution of Eq. (12) can be found with the generalized eigenvalue problem.[20] Those eigenmodes serve to connect the scattered wave to the reflection and transmission waves at port boundaries, while maintaining consistency in the discretised system.

The translationally invariant wave in extended port regions satisfies

$$A\Phi = e^{\eta h} B\Phi, \tag{18}$$

where Φ is a four-dimensional vector defined by $\Phi = [\mathbf{u}_0^{\rm T}, e^{\eta h}\mathbf{u}_0^{\rm T}]^{\rm T}$, and the matrices A and B are given by

$$A = \begin{bmatrix} c_{\rm prt} & O \\ O & I \end{bmatrix}, \quad B = \begin{bmatrix} -b_{\rm prt} & -a_{\rm prt} \\ I & O \end{bmatrix}. \tag{19}$$

Equation (18) is a generalized eigenvalue problem[20] with four eigenvalues $e^{\eta h}$ and eigenvectors $\Phi = [\mathbf{X}^{\rm T}, e^{\eta h}\mathbf{X}^{\rm T}]^{\rm T}$.

Since the extended input/output ports are assumed to be uniform, both η and $-\eta$ are wave constants. Here the wave constant is defined as $\eta = \gamma + ik$ that is composed of the wave number k and the damping/growing constant γ. When the wave constant η is pure imaginary, $\eta = \pm ik$ with a positive k, the corresponding eigenvectors $\mathbf{X}_t^{(\pm)}$ are for travelling waves that propagate in the positive/negative direction of the x-axis according to the double sign. Two remaining wave constants, $\pm\eta$, have non-zero real parts; therefore, the eigenvectors $\mathbf{X}_m^{(\rm grw/dmp)}$ indicate waves whose amplitudes are grown/damped with the rates $\pm{\rm Re}[\eta]$, respectively.

Let us introduce 2×2 matrices by $X_\pm^{(\rm dmp)} = [\mathbf{X}_t^{(\pm)}\mathbf{X}_m^{(\rm dmp)}]$ ($X_\pm^{(\rm grw)} = [\mathbf{X}_t^{(\pm)}\mathbf{X}_m^{(\rm grw)}]$), and define the matrices $K_\pm^{(\rm dmp)}$ and $K_\pm^{(\rm grw)}$ as

$$K_\pm^{(\rm dmp)} = X_\pm^{(\rm dmp)} \begin{bmatrix} e^{\pm ikh} & 0 \\ 0 & e^{-\eta h} \end{bmatrix} (X_\pm^{(\rm dmp)})^{-1}, \tag{20}$$

$$K_\pm^{(\rm grw)} = X_\pm^{(\rm grw)} \begin{bmatrix} e^{\pm ikh} & 0 \\ 0 & e^{\eta h} \end{bmatrix} (X_\pm^{(\rm grw)})^{-1}. \tag{21}$$

These matrices $K_\pm^{(\rm dmp/grw)}$ satisfy Eq. (17) and belong to a type of stepping matrices. The role of $K_\sigma^{(\varsigma)}$ ($\sigma = \pm$, $\varsigma = $ dmp/grw) is dual: (i) decompose the field vector $\mathrm{u}(x_n)$ into components of travelling and damping/growing waves; (ii) multiply the phase factor e^{ikh} or $e^{\eta h}$ according to the travelling or damping/growing waves.

3.1.2 Reflection and transmission coefficients

At input and output ports, the field $\mathbf{u}(x_n)$ in the scattering region must be connected to waves in port regions. By using the stepping matrices $K_\pm^{(\rm dmp/grw)}$, waves in port regions can be expressed as

$$\mathbf{u}(x_n) = \begin{cases} (K_+^{(\rm dmp)})^n \mathbf{u}_{\rm in} + (K_-^{(\rm grw)})^n \mathbf{u}_{\rm rf} & n \le 0 \\ (K_+^{(\rm dmp)})^{(n-N)} \mathbf{u}_{\rm tr} & n \ge N \end{cases}. \tag{22}$$

Here $\mathbf{u}_{\rm in}$, $\mathbf{u}_{\rm rf}$, and $\mathbf{u}_{\rm tr}$ are the vectors composed of the amplitudes of the input, reflection and transmission waves, respectively.

According to Eq. (22), we can obtain the condition on S_n at the boundary of the output port as

$$S_N = K_+^{(\rm dmp)}. \tag{23}$$

Using Eqs. (16) and (22), the field variable $\mathbf{u}(x_1)$ can be expressed by the stepping matrices S_0 and $K_\pm^{(\rm dmp/grw)}$ as

$$S_0(\mathbf{u}_{\rm in} + \mathbf{u}_{\rm rf}) = K_+^{(\rm dmp)}\mathbf{u}_{\rm in} + K_-^{(\rm grw)}\mathbf{u}_{\rm rf}. \tag{24}$$

Here Eq. (22) was assumed to be valid at $n = 1$. Although a strict expression of the port boundary condition (PBC) is possible in continuous systems,[7] it involves mismatch accompanied by discretisation. On the other hand, Eq. (24) provides PBC without any mismatches in discretised systems under the RTM framework. Therefore, it can be termed as the RTM-consistent PBC.

Using Eq. (24) we can express the reflection wave as

$$\mathbf{u}_{\rm rf} = -(S_0 - K_-^{(\rm grw)})^{-1}(S_0 - K_+^{(\rm dmp)})\mathbf{u}_{\rm in}. \tag{25}$$

By transferring the field variable of $n = 0$ with Eq. (16), the transmission wave is expressed as

$$\mathbf{u}_{\rm tr} = S_{N-1}\cdots S_2 S_1 S_0(\mathbf{u}_{\rm in} + \mathbf{u}_{\rm rf}). \tag{26}$$

The reflection and transmission coefficients r and t are found to be $r = \tilde{\mathbf{X}}_{\rm t-}^{(\rm grw)}\mathbf{u}_{\rm rf}$ and $t = \tilde{\mathbf{X}}_{\rm t+}^{(\rm dmp)}\mathbf{u}_{\rm tr}$. Here $\tilde{\mathbf{X}}_{\rm t-}^{(\rm grw)}$ and $\tilde{\mathbf{X}}_{\rm t+}^{(\rm dmp)}$ are the first row vectors of $(X_-^{(\rm grw)})^{-1}$ and $(X_+^{(\rm dmp)})^{-1}$, respectively. The transmission rate T and the reflection rate R are expressed as $R = |r|^2$ and $T = |t|^2$. The energy flux of the system, J, can be defined as $J = -\omega\,{\rm Im}[u^*(\ell(x)u'')' - u'^*\ell(x)u'']$,[21] which can be expressed as $J = 2\sqrt{m\ell}\,\omega k|a|^2$ for the travelling wave with a wave number k and an amplitude a. Therefore, the energy conservation can be expressed as $R + e^{-2\varphi_1}T = 1$.

3.2 Error of discretised wave number

When $\ell(x) = 1$ and $m(x) = m_0$(constant), the continuous system has travelling waves that can be expressed as $u(x) \propto e^{i(m_0)^{1/4}x}$ with the wave number $(m_0)^{1/4}$. Since the eigenvalue problem of Eq. (18) is a quartic equation, the discretised system also has an algebraic expression for travelling waves with a wave number k. The discrete wave number k can be developed in the series with respect to h as $k = m_0^{1/4} - \frac{1}{2880}m_0^{5/4}h^4 + \cdots$. This means that the discrete wave number k approximates the continuous wave number $m_0^{1/4}$ with an error on the h^4 order.

4. Analysis Accuracy of Scattering Problem under RTM Framework

4.1 Discretisation accuracy during resonance

Resonance occurs in the system governed by Eq. (1) when the functions $\ell(x)$ and $m(x)$ have the form as

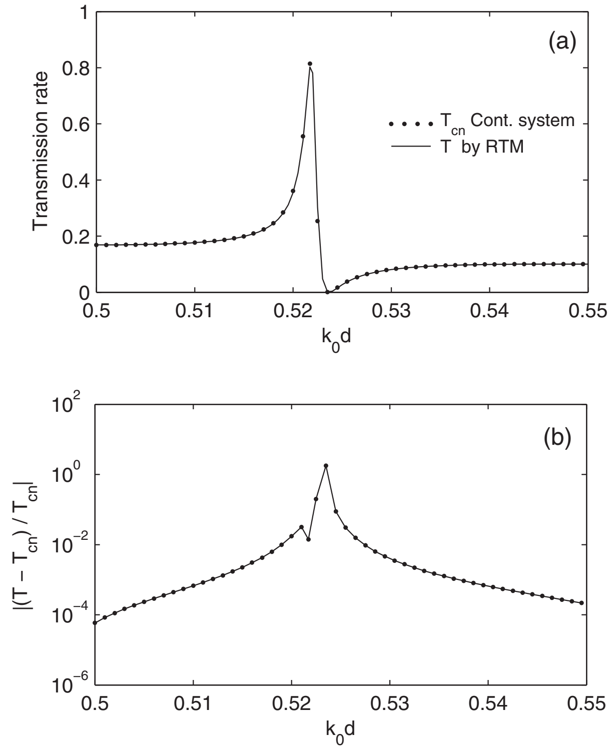

Fig. 1. Resonance curve and its accuracy. (a) Transmission rates T and $T_{\rm cn}$ for the discretised system (solid curve) and continuous system (dots), respectively. (b) The relative error of the transmission rate.

$$\ell(x) = \begin{cases} k_0^{-2}e^{-2\varphi_0} & x < -d/2 \\ [k_0^{-2}/(1+r_b)]e^{-2\varphi_0} & -d/2 < x < 0 \\ [k_0^{-2}/(1+r_b)]e^{-2(\varphi_0+\varphi_1)} & 0 < x < d/2 \\ k_0^{-2}e^{-2(\varphi_0+\varphi_1)} & d/2 < x \end{cases}, \quad (27)$$

$$m(x) = \begin{cases} k_0^{2}e^{-2\varphi_0} & x < -d/2 \\ k_0^{2}(1+r_b)e^{-2\varphi_0} & -d/2 < x < 0 \\ k_0^{2}(1+r_b)e^{-2(\varphi_0+\varphi_1)} & 0 < x < d/2 \\ k_0^{2}e^{-2(\varphi_0+\varphi_1)} & d/2 < x \end{cases}. \quad (28)$$

Here the parameter k_0 is the wave number of the incident wave, and r_b is the modulation factor for the scattering potential defined in Appendix.

Figure 1 shows the k_0 dependence of the transmission rate T in the panel (a) and the relative error in the panel (b). The geometry and physical parameters of the system are as follows: $-x_{\rm in} = x_{\rm out} = 1.2125$, $d = 0.2667$, $N = 97$, $r_b = -2$, $\varphi_0 = 2.1802$, and $\varphi_1 = -0.1$. The resonance curve reaches its maximum and minimum at $k_0d = 0.52184$ and 0.52365, respectively. The lengths and the segmentation number N were defined so that the boundary of the scattering region $\pm d/2$ is on any of the segmentation points x_n while keeping $|x_{\rm in}|$ and $x_{\rm out}$ to be nearly one.

The asymmetric curve in Fig. 1(a) is a typical feature of Fano resonance[17] caused by the interaction between an incident wave and a quasi-localised wave. The extraction of quasi-localised wave is discussed in the following Sect. 4.2.1. The solid curve was obtained by RTM in the discretised system and the dots were obtained by an analytic method in the continuous system. The derivation of the analytic expression is summarized in Appendix. Using the values of the continuous system, $T_{\rm cn}$, the error of the discretised system can be evaluated by the absolute value of $(T - T_{\rm cn})/T_{\rm cn}$, as shown in Fig. 1(b). Since $T_{\rm cn}$ is very small when $k_0d \approx 0.52365$, the relative error tends to be large. However, the error is less than 10^{-4} when k_0d is beyond this range.

4.2 *Quasi-localised wave*

4.2.1 *Eigenvalue problem for localised waves*

We have developed a novel method of extracting a quasi-localised wave while keeping consistency under the RTM framework. Substituting the function $m(x)$ by $k_{0\rm pr}^4 + k_0^2\{m(x)/k_{0\rm pr}^2 - k_{0\rm pr}^2\}$ with the wave number k_0 and its preliminary value $k_{0\rm pr}$, we can separate the coefficients of Eq. (12) into two parts according to whether they are proportional to k_0^2 as $\bar{c}_n \to \bar{c}_n^{(1)} - k_0^2\bar{c}_n^{(2)}$, $\bar{b}_n \to \bar{b}_n^{(1)} - k_0^2\bar{b}_n^{(2)}$, and $\bar{a}_n \to \bar{a}_n^{(1)} - k_0^2\bar{a}_n^{(2)}$. When $k_0 = k_{0\rm pr}$ both sides match exactly. Thus Eq. (12) can be expressed as

$$\bar{c}_n^{(1)}\mathbf{u}(x_{n-1}) + \bar{b}_n^{(1)}\mathbf{u}(x_n) + \bar{a}_n^{(1)}\mathbf{u}(x_{n+1}) = k_0^2\{\bar{c}_n^{(2)}\mathbf{u}(x_{n-1}) + \bar{b}_n^{(2)}\mathbf{u}(x_n) + \bar{a}_n^{(2)}\mathbf{u}(x_{n+1})\}, \quad (29)$$

for $0 \le n \le N$. If $2(N+1)$-dimensional vector $\mathbf{U}_{\rm tot}$ is introduced as $\mathbf{U}_{\rm tot} = [\mathbf{u}(x_0)^{\rm T}, \mathbf{u}(x_1)^{\rm T}, \mathbf{u}(x_2)^{\rm T}, \ldots, \mathbf{u}(x_N)^{\rm T}]^{\rm T}$, Eq. (29) serves as an eigenvalue problem with the eigenvalue k_0^2. Using the boundary conditions

$$\mathbf{u}(x_{-1}) = (K_-^{\rm (grw)})^{-1}\mathbf{u}(x_0), \quad (30)$$

$$\mathbf{u}(x_{N+1}) = K_+^{\rm (dmp)}\mathbf{u}(x_N), \quad (31)$$

we can eliminate the two vectors $\mathbf{u}(x_{-1})$ and $\mathbf{u}(x_{N+1})$, which appear when $n = 0$ and N, respectively, and belong outside of the analysing region. These conditions are another type of RTM-consistent PBC for expressing that scattered waves are perfectly absorbed in port regions without any reflection. Since the stepping matrices $K_\pm^{\rm (dmp/grw)}$ are defined using the second-order difference equation (12), Eqs. (30) and (31) are consistent with the RTM procedure and waves in the analysis domain can be seemlessly connected to eigenmodes in the infinite input/output regions. Furthermore, the RTM-consistent PBC enables us for the first time to extract a localised wave using the procedure of the eigenvalue problem as discussed in the latter half of this section.

The eigenvalue k_0^2 is found using the eigenvalue problem being defined by Eq. (29) on the assumption that the stepping matrices $K_+^{\rm (tmp)}$ and $K_-^{\rm (grw)}$ are defined by the preliminary value $k_{0\rm pr}$. The consistency between k_0 and $k_{0\rm pr}$ is realized with the iterative use of the eigenvalue k_0 for the preliminary $k_{0\rm pr}$.

Figure 2 shows the quasi-localised wave obtained with eleven iterations about k_0. The difference of k_0 between the last successive two iterations is bounded to 10^{-7} in magnitude. The oscillation of the localised wave is shown using several curves of different phase factors $e^{i\alpha}$ ($\alpha = 0.25\pi \cdot p, p = 0, 1, \ldots, 7$). When the single cycle $T (= 2\pi/\omega)$ passes, the phase α increases by 2π and the localised wave returns to its initial state. Not only damping wave tails but also travelling wave skirts reach both ends of the simulation domain, $x = x_{\rm in}, x_{\rm out}$; however, no wave disturbance appears because the RTM-consistent PBC works effectively.

Since travelling wave skirts convey powers and result in a finite lifetime of the quasi-localised wave, the wave number

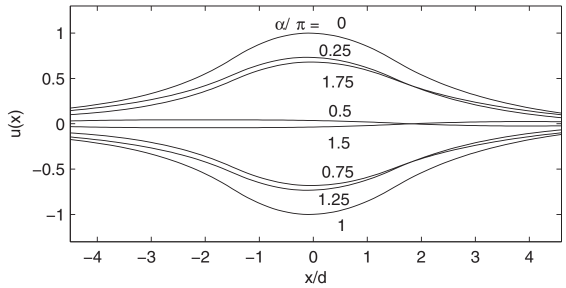

Fig. 2. Localised wave causing Fano resonance.

k_L derived from eigenvalue k_0^2 has an imaginary part expressed as

$$k_L d = 0.52213 + i0.00066. \tag{32}$$

4.2.2 *Phase shift and semi-analytic fitting with k_L*

To understand the meaning of the complex frequency in Eq. (32), we made an analogy based on the scattering theory of the Schrödinger equation.[22] The reflection and transmission coefficients are analytic functions of the input wave umber k_0, and the resonance curve is determined by a single pole in the analytically extended k_0-space. The S-matrix can be expressed by

$$S = \begin{bmatrix} r & t' \\ t & r' \end{bmatrix}, \tag{33}$$

where r and t (r' and t') are the reflection and transmission coefficients when the incident wave comes from $x = -\infty$ ($x = \infty$). Since the system conserves energy, the S-matrix is unitary and satisfies $\det S = e^{i2\delta(k_0)}$ with a real phase shift $\delta(k_0)$.

Regarding the complex wave number k_L as a single pole in the k_0-space, the quantity $e^{i2\delta(k_0)}$ can be approximated as:[23]

$$e^{i2\delta(k_0)} \approx e^{i2\delta_{\mathrm{bg}}(k_0)} \frac{k_0 - k_L^*}{k_0 - k_L}, \tag{34}$$

where $*$ represents the complex conjugate and $\delta_{\mathrm{bg}}(k_0)$ is a background phase that appears when there are no scatterers. Defining the phase shift $\delta_{\mathrm{res}}(k_0)$ caused by the pole as $e^{i2\delta_{\mathrm{res}}(k_0)} = (k_0 - k_L^*)/(k_0 - k_L)$ and using the relation

$$\delta_{\mathrm{res}}(k_0) = \cot^{-1}\left(\frac{k_0 - \mathrm{Re}[k_L]}{\mathrm{Im}[k_L]}\right), \tag{35}$$

the phase shift $\delta(k_0)$ of the continuous system can be estimated by $\delta_{\mathrm{bg}}(k_0) + \delta_{\mathrm{res}}(k_0)$. This is a semianalytic expression of the phase shift derived by a single pole model. The real and imaginary parts of k_L indicate the resonance centre and width, respectively.

Figure 3 shows k_0 dependence of the phase shifts. In panel (a), the dotted line is the background phase shift $\delta_{\mathrm{bg}}(k_0)$ obtained by the linear fitting of values in the region $k_0 d < 0.511$. The phase shift $\delta(k_0)$ derived from the continuous system is well approximated by $\delta_{\mathrm{bg}}(k_0) + \delta_{\mathrm{res}}(k_0)$. Panel (b) shows the discrepancies of $\delta(k_0)$ and $\delta_{\mathrm{bg}}(k_0) + \delta_{\mathrm{res}}(k_0)$. Except for the values near the resonance centre, the discrepancies are sufficiently small for practical use; therefore, it convinces us of the validity of the complex frequency.

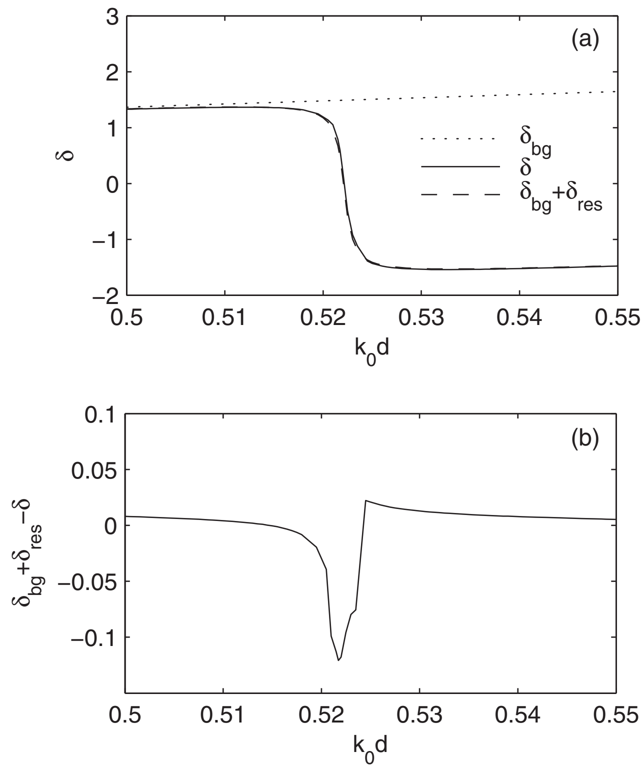

Fig. 3. Tracing of the phase shift $\delta(k_0)$ with the background shift $\delta_{\mathrm{bg}}(k_0)$ and the shift $\delta_{\mathrm{res}}(k_0)$ determined by the complex wave number k_L.

5. Conclusions

To extend the application range of RTM, we proposed the weak-form discretisation scheme that enables us to derive the second-order difference equation. This scheme is generally applicable to any system being formulated with the weak-form theory framework. The RTM-consistent PBC was also proposed to express the perfect matching between scattered waves and port modes while maintaining consistency under the RTM framework. This PBC is not always strict in continuous systems; however, it involves no spurious reflection in discretised systems even if damping tails or propagating wave skirts from a localised/quasi-localised wave reach port boundaries.

Provided that the frequencies are far from the resonance centre, the relative error of transmission rate obtained by RTM is less than 10^{-4}. In practical sense, the discretised system has sufficient accuracy because the system can predict the resonance centre and the phase shift concerning Fano resonance. In particular, the quasi-localised wave can be extracted by using a nonreflecting feature of RTM-consistent PBC.

Acknowledgment

This study was supported by KAKENHI Grant Number 15K04752.

Appendix: Transmittance of the Continuous System

Since the functions $\ell(x)$ and $m(x)$ have elementary forms, we can obtain analytic values of the transmission rate T_{cn}. By introducing the quantity defined by $v(x) = \ell(x)u''(x)$ and the column vector $\mathbf{u}(x) = [u(x)\ v(x)]^{\mathrm{T}}$, the governning equation can be transformed into the matrix form as

$$\mathbf{u}'' = k^2 M\mathbf{u}, \tag{A·1}$$

where

$$M(x) = \begin{bmatrix} 0 & 1/\sqrt{m(x)\ell(x)} \\ \sqrt{m(x)\ell(x)} & 0 \end{bmatrix}, \tag{A·2}$$

$$k^2(x) = \sqrt{\frac{m(x)}{\ell(x)}}. \tag{A·3}$$

Using Eqs. (27) and (28), the composite functions $\sqrt{m(x)/\ell(x)}$ and $\sqrt{m(x)\ell(x)}$ can be expressed as

$$\sqrt{\frac{m(x)}{\ell(x)}} = \begin{cases} k_0^2 & |x| > d/2 \\ k_0^2(1 + r_b) & |x| < d/2 \end{cases}, \tag{A·4}$$

$$\sqrt{m(x)\ell(x)} = \begin{cases} e^{-2\varphi_0} & x < 0 \\ e^{-2(\varphi_0+\varphi_1)} & x > 0 \end{cases}. \tag{A·5}$$

Furthermore, using the matrix $Q(x)$ defined by

$$Q(x) = \begin{bmatrix} 1 & 1 \\ \sqrt{m(x)\ell(x)} & -\sqrt{m(x)\ell(x)} \end{bmatrix}, \tag{A·6}$$

and transforming the vector $\mathbf{u}(x)$ into $\mathbf{U}(x) = Q^{-1}\mathbf{u}(x)$, we can derive two equations of the Schrödinger type as

$$-u_1'' + \mu(x)u_1 = -k_0^2 u_1, \tag{A·7}$$

$$-u_2'' - \mu(x)u_2 = k_0^2 u_2, \tag{A·8}$$

where u_1 and u_2 are first and second elements of the vector $\mathbf{U}$, respectively. The function $\mu(x)$ is the box-type potential defined by

$$\mu(x) = \begin{cases} 0 & |x| > d/2 \\ k_0^2 r_b & |x| < d/2 \end{cases}. \tag{A·9}$$

In Fig. A·1, spatial dependences of the first and second component are illustrated using an analogy of the quantum particle possessing the wave function within the potential function $\mu(x)$. Since the first component represents a particle in the potential well, its wave tails penetrate the input/output port regions beyond the potential well. On the other hand, the second component corresponds to a free particle that is scattered by the potential barrier. The input, reflection and transmission waves governed by Eq. (1) are expressed using these wave skirts appearing in the input/output port regions. Under the scattering problem of the Schrödinger type equation, the incident wave must have a positive energy similar to the particle with the energy k_0^2, as shown in panel (b); the localised wave never appears regardless of whether the potential type is a well or a barrier. However, the wave of the fourth-order differential equation always has the localised wave components as shown in panel (a). This is the remarkable feature of the system governed by the fourth-order differential equation and plays an important role in the appearance of the Fano effect.

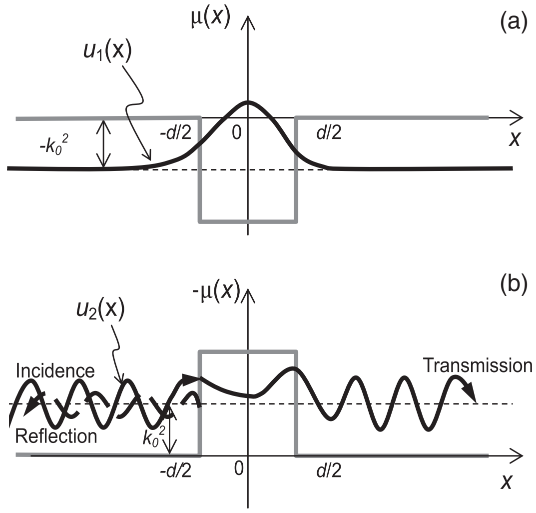

Fig. A·1. Coupled wave components of the Schrödinger type governed by the fourth-order differential equation. (a) First component of the localised wave trapped in the potential well. (b) Second component of travelling waves reflected and transmitted with the potential barrier.

Since the composite functions $\sqrt{m(x)/\ell(x)}$ and $\sqrt{m(x)\ell()x}$ are almost constant except for stepwise changes at $x = 0$ and $\pm d/2$, the wave components can be expressed by the superposition of the fundamental solutions as follows:

$$u_1(x) = \begin{cases} b_0 e^{k_0 x} & x < -d/2 \\ a_{1+}e^{ik_1 x} + a_{1-}e^{-ik_1 x} & -d/2 < x < 0 \\ a_{2+}e^{ik_1 x} + a_{2-}e^{-ik_1 x} & 0 < x < d/2 \\ b_3 e^{-k_0 x} & x > d/2 \end{cases}, \tag{A·10}$$

$$u_2(x) = \begin{cases} a_{\mathrm{in}}e^{ik_0 x} + a_{\mathrm{rf}}e^{-ik_0 x} & x < -d/2 \\ b_{1+}e^{k_1' x} + b_{1-}e^{-k_1' x} & -d/2 < x < 0 \\ b_{2+}e^{k_1' x} + b_{2-}e^{-k_1' x} & 0 < x < d/2 \\ a_{\mathrm{tr}}e^{ik_0 x} & |x| < d/2 \end{cases}. \tag{A·11}$$

Here k_1 is defined by $k_1 = k_0|1 + r_b|^{1/2}$, which is the wave number modulated by the potential $\mu(x)$. The coefficients for travelling waves are denoted by a_{in}, a_{rf}, a_{tr}, $a_{1\pm}$, and $a_{2\pm}$, and the coefficients for the damping/growing waves are denoted as b_0, $b_{1\pm}$, $b_{2\pm}$, and b_3. These twelve coefficients except the amplitude of the incident wave, a_{in}, can be determined by the boundary conditions at $x = 0$ and $\pm d/2$ as follows:

$$\lim_{\epsilon\to 0}[Q(0-\epsilon)U(0-\epsilon) - Q(0+\epsilon)U(0+\epsilon)] = \mathbf{0}, \tag{A·12}$$

$$\lim_{\epsilon\to 0}[Q(0-\epsilon)U'(0-\epsilon) - Q(0+\epsilon)U'(0+\epsilon)] = \mathbf{0}, \tag{A·13}$$

$$\lim_{\epsilon\to 0}\left[Q\left(\frac{\pm d}{2}-\epsilon\right)U\left(\frac{\pm d}{2}-\epsilon\right) - Q\left(\frac{\pm d}{2}+\epsilon\right)U\left(\frac{\pm d}{2}+\epsilon\right)\right] = \mathbf{0}, \tag{A·14}$$

$$\lim_{\epsilon\to 0}\left[Q\left(\frac{\pm d}{2}-\epsilon\right)U'\left(\frac{\pm d}{2}-\epsilon\right) - Q\left(\frac{\pm d}{2}+\epsilon\right)U'\left(\frac{\pm d}{2}+\epsilon\right)\right] = \mathbf{0}. \tag{A·15}$$

The components $u_1(x)$ and $u_2(x)$ do not interact with each other when $\varphi_1 = 0$ or the composite function $\sqrt{m(x)\ell(x)}$ has no stepwise change. The interaction is induced so as to satisfy the boundary conditions Eqs. (A·12) and (A·13) with a nonzero φ_1. The reflection and transmission rates are expressed by $R = |a_{\mathrm{rf}}/a_{\mathrm{in}}|^2$ and $T = |a_{\mathrm{tr}}/a_{\mathrm{in}}|^2$, respectively.

1) F. Y. Hajj, H. Kobeisse, and N. R. Nassif, J. Comput. Phys. **16**, 150 (1974).
2) J. A. Appelbaum and D. R. Hamann, Phys. Rev. B **6**, 2166 (1972).
3) K. Hirose and M. Tsukada, Phys. Rev. B **51**, 5278 (1995).
4) G. Biczô, Can. J. Chem. **63**, 1992 (1985).
5) H. Kato and Y. Kanno, Jpn. J. Appl. Phys. **47**, 4846 (2008).
6) H. Kato and H. Kato, IEICE Trans. Fundam. Electron. Commun. Comput. Sci. **E97.A**, 1720 (2014).
7) Z. Lou and J.-M. Jin, IEEE Trans. Microwave Theory Tech. **53**, 3014 (2005).
8) R. L. Higdon, Math. Comput. **47**, 437 (1986).
9) J. P. Berenger, J. Comput. Phys. **114**, 185 (1994).
10) M. Kuzuoglu and R. Mittra, IEEE Microwave Guided Wave Lett. **6**, 447 (1996).
11) F. D. Hastings, B. Schneider, and S. L. Broschat, J. Acoust. Soc. Am. **100**, 3061 (1996).
12) K. Y. Fong, L. Fan, L. Jiang, X. Han, and H. X. Tang, Phys. Rev. A **90**, 051801(R) (2014).
13) M. C. Cross and R. Lifshitz, Phys. Rev. B **64**, 085324 (2001).
14) B. A. Glavin, Phys. Rev. Lett. **86**, 4318 (2001).
15) C. Kloeffel, M. Trif, and D. Loss, Phys. Rev. B **90**, 115419 (2014).
16) E. H. El Boudouti, T. Mrabti, H. Al-Wahsh, B. Djafari-Rouhani, A. Akjouj, and L. Dobrzynski, J. Phys.: Condens. Matter **20**, 255212 (2008).
17) U. Fano, Phys. Rev. **124**, 1866 (1961).
18) A. E. Miroshnichenko, Rev. Mod. Phys. **82**, 2257 (2010).
19) P. Solín, *Partial Differential Equations and the Finite Element Method* (Wiley, Hoboken, U.K., 2006).
20) L. Ramdas Ram-Mohan, *Finite Element and Boundary Element Applications in Quantum Mechanics* (Oxford University Press, Oxford, U.K., 2002).
21) Yu. I. Bobrovnitskii, J. Sound Vib. **194**, 103 (1996).
22) J. R. Taylor, *Scattering Theory* (Wiley, New York, 1972).
23) K. Shimamura, Shototsu **2**, 6 (2005) [in Japanese].